JrnlID 10444_ArtID 9482_Proof#1 - 07/09/2016

Adv Comput Math
DOI 10.1007/s10444-016-9482-z

Null space correction and adaptive model order reduction in multi-frequency Maxwell's problem

Michal Kordy[1] **· Elena Cherkaev**[1] **·**
Philip Wannamaker[2]

Received: 7 August 2015 / Accepted: 4 September 2016

Abstract A model order reduction method is developed for an operator with a non-empty null-space and applied to numerical solution of a forward multi-frequency eddy current problem using a rational interpolation of the transfer function in the complex plane. The equation is decomposed into the part in the null space of the operator, calculated exactly, and the part orthogonal to it which is approximated on a low-dimensional rational Krylov subspace. For the Maxwell's equations the null space is related to the null space of the curl. The proposed null space correction is related to divergence correction and uses the Helmholtz decomposition. In the case of the finite element discretization with the edge elements, it is accomplished by solving the Poisson equation on the nodal elements of the same grid. To construct the low-dimenensional approximation we adaptively choose the interpolating frequencies, defining the rational Krylov subspace, to reduce the maximal approximation error.

Communicated by: Carlos Garcia-Cervera

We acknowledge the support of this work from the U.S. Dept. of Energy under contract DE-EE0002750 to PW. EC acknowledges the partial support of the U.S. National Science Foundation through grant DMS-1413454.

✉ Michal Kordy
kordy@math.utah.edu

Elena Cherkaev
elena@math.utah.edu

Philip Wannamaker
pewanna@egi.utah.edu

[1] Department of Mathematics, University of Utah, 155 S 1400 E JWB 233, Salt Lake City, UT 84112-0090, USA

[2] Energy, Geoscience Institute, University of Utah, 423 Wakara Way, Suite 300, Salt Lake City, UT 84108, USA

We prove that in the case of an adaptive choice of shifts, the matrix spanning the approximation subspace can never become rank deficient. The efficiency of the developed approach is demonstrated by applying it to the magnetotelluric problem, which is a geophysical electromagnetic remote sensing method used in mineral, geothermal, and groundwater exploration. Numerical tests show an excellent performance of the proposed methods characterized by a significant reduction of the computational time without a loss of accuracy. The null space correction regularizes the otherwise ill-posed interpolation problem.

Keywords Rational Krylov subspace · Model order reduction · Helmholtz decomposition · Frequency-domain Maxwell system

Mathematics Subject Classification (2010) 30E10 · 41A20 · 41A05 · 35A40 · 65M60 · 86-08

1 Introduction

We consider an approximation of the transfer function

$$\tilde{h}(s) = (\tilde{A} + s\tilde{B})^{-1}\tilde{b}$$

for real valued symmetric matrices $\tilde{A}, \tilde{B}$. We assume that $\tilde{A}$ is a nonnegative definite matrix and $\tilde{B}$ is a positive definite matrix. The approximation is through a model order reduction (MOR), for which the low dimensional subspace is created using a rational Krylov subspace. In application to the Maxwell's equations, matrix $\tilde{A}$ has a large null space as it arises from a discretization of an operator that has a significant null space related to the null space of the curl. We propose a null space correction method that is based on a decomposition of $\tilde{b}$ into the part in the null space and the part orthogonal to it. The part of the transfer function lying in the null space is calculated exactly. The part orthogonal to the null space is approximated using the model order reduction. This approach regularizes the interpolation problem in the same way as the divergence correction regularizes the calculation of the electromagnetic field at low frequencies by enforcing the differential equation on the null space of the curl [24]. In the considered application this decomposition is performed using the discrete Helmholtz decomposition. The suggested correction is not limited to the considered application and can be applied to any operator with a null space. Traditionally MOR approach has been applied to $\tilde{b}$ not dependent on s. In this paper we extend the techniques to the case of $\tilde{b}$ dependent on s. The developed algorithm adaptively chooses the interpolating shifts, which are added one by one adaptively in a greedy fashion, ie. the new shift is at the maximum of the error indicator, for which we use the relative residual norm. This algorithm allows for a very accurate approximation with a small number of interpolation points. We prove that the matrix spanning the subspace can never become rank deficient and thus the algorithm never fails.

Model order reduction is a powerful technique that allows to reduce the dimensionality of a problem, it is especially efficient when the low dimensional subspace is generated using rational Krylov subspaces. This approach has become popular recently and has been used in a variety of contexts [1–3, 9, 12–15, 27, 31–33]. The efficiency of the method is amplified significantly by an optimal selection of the shifts for generating the rational Krylov subspace. For a particular matrix with uniform spectrum, the problem of selection of the optimal shifts has been investigated in [26, 34, 35]. However, such a selection is not optimal for matrices with non-uniform spectrum. An excellent review of this topic is presented in [17].

A different approach, in which the shifts are added one by one in a greedy fashion, was developed in [4, 6]. In this approach, the shifts are adapted to the spectrum of the matrix. The authors of [6] consider an adaptive choice of shifts for the approximation of the transfer function using rational Krylov subspaces, with an application to a time-domain electromagnetic geophysical forward problem. This adaptive choice of the shifts was later generalized to non-symmetric matrices [7] and to an approximation of matrix functions other than the transfer function [18]. Numerical simulations in [6, 18] show that the adaptive approach gives better results than the choice of the shifts that do not depend on the spectrum of the operator. Moreover, they demonstrate that the number of required shifts does not increase with the size of the system, and it is not strongly dependent on the spectrum. Those results encourage us to pursue an adaptive choice of the shifts in the current work.

The application under consideration is the forward problem of magnetotellurics (MT) which is a frequency domain electromagnetic remote-sensing geophysical method. It has applications in mineral, geothermal and groundwater exploration. Numerically simulating the scattering of diffusive EM waves from complex three-dimensional (3D) structure is a computationally demanding problem [5, 10, 22]. In particular, the scattering response usually needs to be calculated over a broad frequency range. Typically this may be five orders of magnitude or more with frequency sampling of 5-10 base points per decade. Considerable savings in computational time could result if an accurate method of interpolation of responses across a coarser selection of base points is achieved.

In the considered case, the operator has a non-empty null space and the right hand side, b, depends on s. Moreover, discretization of the curl-curl operator in Maxwell's equations results in a significant null space of the matrix $\tilde{A}$. To deal with this, we propose a method, which we call the null space correction, that enforces the approximation to be exact on the null space. This method regularizes the interpolation problem and allows to reduce the maximum relative error of approximation by two to four orders of magnitude. To evaluate the forward response we use edge element [16, 24, 29] discretization of Maxwell's equations in the frequency domain. In this case the null space correction can be obtained using discrete Helmholtz decomposition. The null space of $\tilde{A}$ is defined using nodal elements on the same mesh, similarly to the divergence correction [11, 24, 25, 30, 36, 37, 39]. In the considered application $\tilde{B}$ is a mass matrix in the edge element space weighted with electrical conductivity σ and thus is a symmetric positive definite matrix, which makes our situation different from the case of [8, 41], where $\tilde{B} = I$. As the error indicator we use the relative residual norm considered in [40]. The efficiency of the developed techniques is higher for larger number of frequencies in MT survey. In our numerical tests, the speedup is 2 times for 30 frequencies.

The paper is organized as follows. In Section 2 we present the theory of the approximation of the transfer function using rational Krylov subspaces. Then we propose the null space correction method. In Section 3 we describe the considered application, present the details of the null space correction, and show how it is related to the divergence correction. In Section 4 we present an algorithm for an adaptive choice of shifts using the relative residual norm and we prove that this algorithm can never fail. In Section 5 we show the results of numerical simulations.

2 Theory

2.1 The model order reduction

We are interested in an approximation of the expression

$$\tilde{h}(s) = (\tilde{A} + s\tilde{B})^{-1}\tilde{b} \tag{1}$$

A reader interested in seeing an example of a practical problem where (1) arises is encouraged to read Section 3.1, which can be read independently. The section describes an electromagnetic geophysical sounding called magnetotellurics where the discretized matrix has a significant null space related to the null space of the curl.

The shift $s = i\omega$ is chosen for a finite number of frequencies ω. In magnetotellurics, those frequencies are usually log-uniformly distributed in an interval $[\omega_{\min}, \omega_{\max}]$. We consider $\tilde{b}$ dependent on s and complex valued. We assume that matrix $\tilde{A}$, is $N \times N$, real valued, symmetric, nonnegative definite, with a non trivial null space. Matrix $\tilde{B}$, is assumed to be $N \times N$, real valued, symmetric, positive definite.

We consider an approximation of Eq. 1 using model order reduction method and rational Krylov subspaces [1–3, 6, 8, 9, 12–15, 20, 27, 31–33, 41].

Let us start with the equation satisfied by $\tilde{h}$:

$$(\tilde{A} + s\tilde{B})\tilde{h} = \tilde{b} \tag{2}$$

Consider $\tilde{V}$, which is an $N \times n$ matrix ($n \ll N$) whose columns span the space

$$\operatorname{colsp}(\tilde{V}) = \operatorname{span}\left\{(\tilde{A} + s_1\tilde{B})^{-1}\tilde{b}, (\tilde{A} + s_2\tilde{B})^{-1}\tilde{b}, \ldots, (\tilde{A} + s_n\tilde{B})^{-1}\tilde{b}\right\} \tag{3}$$

for some chosen complex values $s_1, \ldots, s_n$, which satisfy

$$s_i \neq s_j \text{ if } i \neq j \tag{4}$$

As $\tilde{A}$ is nonnegative definite and $\tilde{B}$ is positive definite, eigenvalues of $\tilde{B}^{-\frac{1}{2}}\tilde{A}\tilde{B}^{-\frac{1}{2}}$ are in $[0, \infty)$. Thus, in order for the Eq. 1 to have a solution, we assume that

$$s,\ s_j \notin (-\infty, 0] \tag{5}$$

We consider an approximation of the solution of Eq. 2 by a vector in $\operatorname{colsp}(\tilde{V})$, namely $\tilde{h}_{\tilde{V}} = \tilde{V}\beta$, for $\beta \in \mathbb{C}^n$ and make the residual orthogonal to $\operatorname{colsp}(\tilde{V})$. This results in an equation for β:

$$\tilde{V}^*(\tilde{A} + s\tilde{B})(\tilde{V}\beta) = \tilde{V}^*\tilde{b} \tag{6}$$

Theorem 1 below states the conditions when the equation has a unique solution. In this case we obtain the approximation $\tilde{h}_{\tilde{V}}(s) = \tilde{V}\beta$ to $\tilde{h}(s)$:

$$\tilde{h}_{\tilde{V}}(s) = \tilde{V}\left(\tilde{V}^*(\tilde{A} + s\tilde{B})\tilde{V}\right)^{-1}\tilde{V}^*\tilde{b} \tag{7}$$

As $n \ll N$, Eq. 6 is much easier to solve than Eq. 2. In a simplest case $s_j = \mathrm{i}\omega_j$, for $\omega_j \in [\omega_{\min}, \omega_{\max}]$. In this case $\omega_1, \ldots, \omega_n$ may be called interpolating frequencies and $s_1, \ldots, s_n$ may be called interpolating shifts as the following theorem holds:

Theorem 1 *If the matrix $\tilde{V}$ satisfying* Eq. 3 *is full rank, then for $s \in \mathbb{C}$, the solution to* Eq. 6 *exists and is unique. Moreover,*

$$\tilde{h}_{\tilde{V}}(s_j) = \tilde{h}(s_j), \quad j = 1, \ldots, n \tag{8}$$

Proof First we show that the matrix in Eq. 6 is not singular. Indeed

$$\tilde{V}^*(\tilde{A} + s\tilde{B})\tilde{V} = \tilde{V}^*\tilde{A}\tilde{V} + s\tilde{V}^*\tilde{B}\tilde{V} = A_1 + sB_1$$

As $\tilde{V}$ is full rank and $\tilde{A}$ is symmetric nonnegative definite, A_1 is hermitian, nonnegative definite. Similarly as $\tilde{B}$ is symmetric positive definite, B_1 is hermitian positive definite. Thus the matrix may be written as:

$$A_1 + sB_1 = B_1^{\frac{1}{2}}\left(B_1^{-\frac{1}{2}}A_1B_1^{-\frac{1}{2}} + sI\right)B_1^{\frac{1}{2}}$$

with $B_1^{\frac{1}{2}}$ symmetric, invertible. Matrix $B_1^{-\frac{1}{2}}A_1B_1^{-\frac{1}{2}}$ is hermitian, nonnegative definite, so it has real, nonnegative eigenvalues $a_1, \ldots, a_n$. As a result the eigenvalues of $B_1^{-\frac{1}{2}}A_1B_1^{-\frac{1}{2}} + sI$ are $a_1 + s, \ldots, a_n + s$. With the assumption (5) that $s \notin (-\infty, 0]$, none of the eigenvalues $a_i + s$ can be equal to zero, thus matrix $B_1^{-\frac{1}{2}}A_1B_1^{-\frac{1}{2}} + sI$ is invertible and so is $A_1 + sB_1$ as a product of invertible matrices. We have proven that Eq. 6 has a unique solution.

Next notice that because of Eq. 3, for each j, there is β_j such that

$$\tilde{V}\beta_j = (\tilde{A} + s_j\tilde{B})^{-1}\tilde{b}$$

Thus β_j satisfies Eq. 6 for $s = s_j$. This implies

$$\tilde{h}_{\tilde{V}}(s_j) = \tilde{V}\beta_j = (\tilde{A} + s_j\tilde{B})^{-1}\tilde{b} = \tilde{h}(s_j) \tag{9}$$

□

We prove in Section 4.1 that if an adaptive algorithm is used, then matrix $\tilde{V}$ can never become rank deficient.

2.2 A relationship with $(A + sI)^{-1}b$

Let us relate our problem to the situation when $\tilde{B}$ is an identity matrix I. We define

$$A = \tilde{B}^{-\frac{1}{2}}\tilde{A}\tilde{B}^{-\frac{1}{2}}, \quad b = \tilde{B}^{-\frac{1}{2}}\tilde{b}, \quad h(s) = (A + sI)^{-1}b \tag{10}$$

and rewrite $\tilde{h}(s)$ as

$$\tilde{h}(s) = (\tilde{A} + s\tilde{B})^{-1}\tilde{b} = \tilde{B}^{-\frac{1}{2}}(A + sI)^{-1}b = \tilde{B}^{-\frac{1}{2}}h(s) \tag{11}$$

Moreover, for a matrix V defined as $V = \tilde{B}^{\frac{1}{2}}\tilde{V}$,

$$\text{colsp}(V) = \text{span}\left\{(A + s_1 I)^{-1}b, (A + s_2 I)^{-1}b, \ldots, (A + s_n I)^{-1}b\right\} \tag{12}$$

Notice that a particular form of $\tilde{V}$ does not matter, as long as Eq. 3 is satisfied. So to make the presentation easier, we will assume that columns of V are orthonormal. With this assumption we obtain

$$\tilde{V}^*\tilde{A}\tilde{V} = V^*AV, \quad \tilde{V}^*\tilde{B}\tilde{V} = V^*V = I \tag{13}$$

and

$$\tilde{h}_{\tilde{V}}(s) = \tilde{V}\left(\tilde{V}^*(\tilde{A} + s\tilde{B})\tilde{V}\right)^{-1}\tilde{V}^*\tilde{b} = \tilde{B}^{-\frac{1}{2}}V\left(V^*(A + sI)V\right)^{-1}V^*b = \tilde{B}^{-\frac{1}{2}}h_V(s) \tag{14}$$

Combining Eqs. 11 and 14 together allows us to relate the error of approximation of $\tilde{h}(s)$ to the error of approximation $h(s)$:

$$\tilde{h}(s) - \tilde{h}_{\tilde{V}}(s) = \tilde{B}^{-\frac{1}{2}}(h(s) - h_V(s)) \tag{15}$$

Consider a diagonalization of A:

$$A = U\Lambda U^* \tag{16}$$

where Λ is a diagonal matrix with eigenvalues λ_k as entries and columns of U are eigenvectors u_k. With this notation, we write $h(s)$ as a vector valued function:

$$h(s) = (A + sI)^{-1}b = \sum_{k=1}^{N} \frac{u_k(u_k^*b)}{\lambda_k + s} \tag{17}$$

For $b = b(s)$ analytic, $h(s)$ is an analytic function of s. This analytic function is approximated by $h_V(s)$:

$$h_V(s) = V\left(V^*AV + sI\right)^{-1}V^*b = \sum_{j=1}^{n} \frac{V\gamma_j(\gamma_j^*V^*b)}{\hat{\lambda}_j + s} \tag{18}$$

where $\hat{\lambda}_j$ and γ_j are eigenvalues and eigenvectors of V^*AV. We are approximating an analytic function, with singularities at $s = -\lambda_j$, by a function with a similar structure, having singularities at $s = -\hat{\lambda}_k$.

Intuitively the approximation (18) will be good if $\hat{\lambda}_j$, $V\gamma_j$ $j = 1, \ldots, n$ approximate λ_k, u_k, $k = 1, \ldots, N$ for k such that $u_k^*b \neq 0$. Yet the quality of this approximation depends on the choice of V, which in turn depends on the choice of the interpolating shifts $(s_j)_{j=1}^n$. In this paper we consider an algorithm for choosing shifts $(s_j)_{j=1}^n$ in an optimal way, adapting them to the part of the spectrum of A for which $u_k^*b \neq 0$.

JrnlID 10444_ArtID 9482_Proof#1 - 07/09/2016

2.3 The null space correction

In this section, we present an analysis of the situation when the hermitian matrix A has a nontrivial nullspace and we propose an algorithm that, in the case of b not orthogonal to the null space, leads to a significant improvement in the accuracy of the approximation.

The main idea is based on the theorem below:

Theorem 2 *The transfer function may be represented as a sum of the part $\tilde{h}_{\tilde{K}}(s)$ in the null space of $\tilde{A}$ and the part $\tilde{h}_{\tilde{W}}(s)$ orthogonal to it:*

$$\tilde{h}(s) = \tilde{h}_{\tilde{K}}(s) + \tilde{h}_{\tilde{W}}(s) = \frac{1}{s}(\tilde{K}^*\tilde{B}\tilde{K})^{-1}\tilde{K}^*\tilde{b} + (\tilde{A} + s\tilde{B})^{-1}\tilde{b}_{\tilde{W}} \tag{19}$$

where

$$\tilde{b}_{\tilde{W}} = \tilde{b} - \tilde{B}\tilde{K}(\tilde{K}^*\tilde{B}\tilde{K})^{-1}\tilde{K}^*\tilde{b} \tag{20}$$

and the columns of matrix $\tilde{K}$ are a basis of the null space of $\tilde{A}$:

$$colsp(\tilde{K}) = null(\tilde{A}) \tag{21}$$

We propose to construct an approximation to $\tilde{h}(s)$ as

$$\tilde{h}(s) \approx \tilde{h}_{\tilde{W},\tilde{V}}(s) + \tilde{h}_{\tilde{K}}(s) \tag{22}$$

where $\tilde{h}_{\tilde{K}}(s)$ is calculated exactly and $\tilde{h}_{\tilde{W},\tilde{V}}(s)$ is a model order reduction approximation to $\tilde{h}_{\tilde{W}}(s)$.

Proof of Theorem 2 It is easier to express the essence of the decomposition using the system scaled by $\tilde{B}^{\frac{1}{2}}$. Let

$$K = \tilde{B}^{\frac{1}{2}}\tilde{K} \tag{23}$$

With this notation, we have

$$\mathrm{colsp}(K) = \mathrm{null}(A) \tag{24}$$

Take a matrix W, whose columns are an orthonormal basis of the range of A. Matrix A is hermitian, so its range is orthogonal to its null space, thus:

$$[K\ W]^*[K\ W] = \begin{bmatrix} K^*K & 0 \\ 0 & I \end{bmatrix} \tag{25}$$

Consider a representation of h in the basis of columns of K and W:

$$h = [K\ W]\begin{bmatrix} \alpha_K \\ \alpha_W \end{bmatrix} = K\alpha_K + W\alpha_W = h_K + h_W \tag{26}$$

Using this decomposition, one can rewrite the equation

$$(A + sI)h = b \tag{27}$$

as

$$\begin{cases} W^*(A+sI)(K\alpha_K + W\alpha_W) = W^*b \\ K^*(A+sI)(K\alpha_K + W\alpha_W) = K^*b \end{cases}$$

which is equivalent to two uncoupled equations for α_W and α_K:

$$\begin{cases} (W^*AW + sI)\alpha_W &= W^*b \\ s(K^*K)\alpha_K &= K^*b \end{cases} \tag{28}$$

If b is orthogonal to the null space of A, in which case $K^*b = 0$, then $\alpha_K = 0$ and thus:

$$h(s) = (A+sI)^{-1}b = W(W^*AW + sI)^{-1}W^*b$$

In this case one could modify the matrix eigenvalues on the null space of A in an arbitrary way, and h would be the same. This explains that if $b \perp \text{null}(A)$, then the situation is as if matrix A had a trivial null space.

Let us focus on the situation when b is not orthogonal to the null space of A. One can solve the second equation in Eq. 28 obtaining

$$h_K(s) = K\alpha_K = \frac{1}{s}K(K^*K)^{-1}K^*b \tag{29}$$

Finding h_W may be done by solving the first equation in Eq. 28, or equivalently by solving the original Eq. 27 with a modified right hand side, consisting only of the component b_W in the range of A:

$$(A+sI)h_W = b_W \tag{30}$$

where

$$b_W = b - K(K^*K)^{-1}K^*b \tag{31}$$

One obtains the hypothesis by using the scaling by $\tilde{B}^{\frac{1}{2}}$ of Eqs. 23 and 10 and defining:

$$\tilde{b}_{\tilde{W}} = \tilde{B}^{\frac{1}{2}}b_W,\ \ \tilde{b}_{\tilde{K}} = \tilde{B}^{\frac{1}{2}}b_K,\ \ \tilde{h}_{\tilde{K}} = \tilde{B}^{-\frac{1}{2}}h_K,\ \ \tilde{h}_{\tilde{W}} = \tilde{B}^{-\frac{1}{2}}h_W,\ \ \tilde{W} = \tilde{B}^{-\frac{1}{2}}W \tag{32}$$

Notice that with those definitions, colsp$(\tilde{B}\tilde{W})$ is the range of $\tilde{A}$ and the orthogonality is in the $\tilde{B}$ or $\tilde{B}^{-1}$ weighted inner product:

$$0 = K^*W = \tilde{K}^*\tilde{B}\tilde{W},\quad 0 = h_W^*h_K = \tilde{h}_{\tilde{W}}^*\tilde{B}\tilde{h}_{\tilde{K}},\quad 0 = b_W^*b_K = \tilde{b}_{\tilde{W}}^*\tilde{B}^{-1}\tilde{b}_{\tilde{K}} \tag{33}$$

This completes the proof of Theorem 2. □

The proposed method is especially efficient when the representation of the null space allows for a sparse $\tilde{K}^*\tilde{B}\tilde{K}$ which is possible in the considered application. The details are presented in Section 3.2.

Notice that an algorithm that uses the null-space correction, gives a better approximation of $\tilde{h}(s)$ than an algorithm without the correction. Since $\tilde{h}_K$ is calculated exactly, the model order reduction has to deal with a simpler problem. The location of interpolation frequencies used for approximation of $\tilde{h}_{\tilde{W}}(s)$ need to adapt to a smaller interval (not containing 0) than in the case of $\tilde{h}(s)$.

The null space correction may be applied also in a situation of b not dependent on s. In this case it follows from Eq. 29 that the null space part satisfies $h_K(s) = \frac{1}{s}h_K(1)$. So it is enough to calculate $h_K(1)$, and to scale it to get the value of $h_K(s)$

for any other s. As a result, application of the null space correction in this case is numerically very inexpensive. However, as we show in the numerical section, this method adds numerical stability to the algorithm reducing the error of approximation to a smaller value by at least four orders of magnitude. Yet initially the speed of reducing the error as the shifts are added is similar to the algorithm without the null space correction. The reason is that $h_K(s) = \frac{1}{s}h_K(1)$, so the advantage of using the null space correction is comparable to having only one vector added to V, the vector $h_K(1)$. In the case of b dependent on s, the null space part $h_K(s)$ is not contained in a one dimensional space, so the advantage of applying the proposed null space correction method is much more pronounced even at initial iteration steps. At each step of the iteration, it reduces the relative error of approximation by two orders of magnitude (see Section 5). The proposed null space correction method is related to divergence correction [11, 24, 30, 36, 37, 39] which provides regularization to the ill-posed forward problem (see Section 3.2).

Notice that the null space correction modifies the original problem of solving (27) into a problem of solving Eq. 30. This modified problem may be solved by the same method as the original problem. Thus any method of solving the original problem may be enhanced with the null space correction, making it faster and more numerically stable (see Section 5 for numerical results supporting this claim). This would work for any operator $\tilde{A}$ in Eq. 1 having a null space.

2.4 The magnitude of the source term

In the application to magnetotelluric problem considered later, Eq. 1 comes from a discretization of Maxwell's equation. The source in this equation is due to a plane wave going downwards. The strength of the source term does not matter as the response of the forward problem is a ratio of the electric and magnetic fields. Thus one can define any magnitude of the source $\tilde{b}$ as a function of s. The theorem below says that for the model order reduction with rational Krylov subspaces, the magnitude of the source term plays no role. The relative error of the approximation will be the same, no matter what magnitude is chosen.

Theorem 3 *Let a be any scalar function defined in I, such that $a(s) \neq 0$ for $s \in I$. For any vector valued function $b(s)$, $s \in I$, define*

$$\breve{b}(s) = b(s)a(s)$$

Consider $h(s)$ and $\breve{h}(s)$ satisfying

$$(A + sI)h(s) = b(s)$$
$$(A + sI)\breve{h}(s) = \breve{b}(s)$$

For any distinct interpolating shifts $(s_j)_{j=1}^n$, let V and $\breve{V}$ be defined as

$$colsp(V) = span\{h(s_j) : \ j = 1, \dots, n\}$$
$$colsp(\breve{V}) = span\{\breve{h}(s_j) : \ j = 1, \dots, n\}$$

Model order reduction approximation is defined in a natural way as

$$h_V(s) = V\alpha, \ \text{where } V^*(A + sI)V\alpha = V^*b(s)$$
$$\breve{h}_{\breve{V}}(s) = \breve{V}\breve{\alpha}, \ \text{where } \breve{V}^*(A + sI)\breve{V}\breve{\alpha} = \breve{V}^*\breve{b}(s)$$

Then the relative errors of approximation of $\breve{h}(s)$ *by* $\breve{h}_{\breve{V}}(s)$ *and* $h(s)$ *by* $h_V(s)$ *are the same*

$$\frac{\|\breve{h}_{\breve{V}}(s) - \breve{h}(s)\|}{\|\breve{h}(s)\|} = \frac{\|h_V(s) - h(s)\|}{\|h(s)\|} \tag{34}$$

Proof Using the definition of $h(s)$ and $\breve{h}(s)$, we obtain immediately that

$$\breve{h}(s) = h(s)a(s) \tag{35}$$

This, together with the definition of V and $\breve{V}$ implies

$$\text{colsp}\{V\} = \text{colsp}\{\breve{V}\} \tag{36}$$

which results in

$$\breve{h}_{\breve{V}}(s) = h_V(s)a(s) \tag{37}$$

Relationship (34) is an immediate consequence. □

3 Application to low frequency Maxwell's equations

3.1 A formulation of the magnetotelluric problem

We consider the forward magnetotelluric problem using edge elements' discretization [24, 25]. Assume that a domain Ω includes the air and the earth's subsurface with the earth's surface having non flat topography. In order to calculate the MT response due to an arbitrary 3D conductivity structure $\sigma > 0$ we consider the edge finite element discretization of the equation for the secondary electric field E.

The solution space for the unknown electric field is defined as

$$\mathcal{H}_0(\nabla\times, \Omega) = \left\{F : \Omega \to \mathbb{C}^3, \int_\Omega \left(|F|^2 + |\nabla \times F|^2\right) < \infty, \ \ n \times F|_{\partial\Omega} = 0\right\} \tag{38}$$

Consider Maxwell's equations in the frequency domain for a low frequency ω, where the term $\mathrm{i}\omega\epsilon$, related to the displacement current, is neglected. We denote the angular frequency by ω, the magnetic permeability by μ, and permittivity by ϵ. Most of the developed methods may be adapted to the case when the term $\mathrm{i}\omega\epsilon$ is present. The weak formulation of the problem for the secondary field E has the following form:

$$\int_\Omega \frac{1}{\mu}\nabla \times E \cdot \nabla \times F + \mathrm{i}\omega \int_\Omega \sigma E \cdot F = \int_\Omega -\mathrm{i}\omega(\sigma - \sigma^p)E^p \cdot F \tag{39}$$

for $E, F \in \mathcal{H}_0(\nabla\times, \Omega)$. The source term in Eq. 39 depends on the primary electric field E^p, which is a plane wave traveling in the medium of conductivity σ_p of a 1D earth. The conductivity $\sigma > 0$ is an arbitrary function of position in the 3D domain, with the assumption that $\sigma \approx \sigma_p$ close to the domain boundaries.

The electric field in Ω is represented as a linear combination of the edge shape functions S_i with coefficients ξ_i:

$$E = \sum_{i=1}^{N} \xi_i S_i \tag{40}$$

where $i = 1, \ldots, N$ are the indices of the edges that do not lie on the boundary. By substituting this to Eq. 39 and using S_j as test functions, one obtains a linear system

$$(\tilde{A} + \mathrm{i}\omega\tilde{B})\xi = g \tag{41}$$

$$\tilde{A}_{j,k} = \int_{\Omega} \frac{1}{\mu} \nabla \times S_j \cdot \nabla \times S_k, \quad \tilde{B}_{j,k} = \int_{\Omega} \sigma S_j \cdot S_k \tag{42}$$

$$g_j = g_j(\omega, \sigma) = \int_{\Omega} -\mathrm{i}\omega(\sigma - \sigma^p) E^p \cdot S_j \tag{43}$$

Notice that $\tilde{A}$ is a real valued, symmetric, nonnegative definite matrix, with a significant null space related to the null space of the curl. As we assume that $\sigma > 0$ everywhere in the domain, matrix $\tilde{B}$ is real valued symmetric, positive definite. The right hand side g is complex valued and setting the magnitude of E^p to 1 at the earth's surface, results in g being an analytic function of ω.

The secondary magnetic field H is calculated as

$$H = \frac{-\nabla \times E}{i\omega\mu} \tag{44}$$

The total field E^t, H^t is a sum of the secondary and primary fields:

$$E^t = E + E^p, \quad H^t = H + H^p \tag{45}$$

The MT response is obtained by finding the impedance Z and the tipper K such that

$$\begin{bmatrix} E_x^t \\ E_y^t \\ H_z^t \end{bmatrix} = \begin{bmatrix} Z_{xx} & Z_{xy} \\ Z_{yz} & Z_{yy} \\ K_{zx} & K_{zy} \end{bmatrix} \begin{bmatrix} H_x^t \\ H_y^t \end{bmatrix} \tag{46}$$

is satisfied no matter what the polarization of the primary (E^p, H^p) plane wave is. Notice also that, simplifying a little, one can interpret the magnetotelluric response Z, K as a ratio of the fields. It does not depend on the magnitude of the plane wave E_p used to calculate the fields (compare with Theorem 3).

The numerical tests are done using the lowest order edge hexahedral discretization, however, all the developed methods may be applied to the tetrahedral mesh or higher order edge elements.

The values of the field at a receiver positioned at an arbitrary location $\mathbf{r}$ with respect to the element edges can be approximated via appropriate interpolation. Let $\mathbf{r}$ be inside an element with edges $e_1, \ldots, e_{12}$. Then field E at the location $\mathbf{r}$ is given by

$$E(\mathbf{r}) = \sum_{l=1}^{12} S_{e_l}(\mathbf{r})\xi_{e_l} = \begin{bmatrix} (v_x^E)^T \xi \\ (v_y^E)^T \xi \\ (v_z^E)^T \xi \end{bmatrix} \tag{47}$$

Here v_x^E, v_y^E, v_z^E contain interpolation vectors with at most 12 non-zero values corresponding to x, y and z components of the edge shape functions $S_{e_1}(\mathbf{r}), \ldots, S_{e_{12}}(\mathbf{r})$.

Similarly, the secondary magnetic field $H(\mathbf{r})$, calculated using Eq. 44 at the location $\mathbf{r}$, is given by

$$H(\mathbf{r}) = \sum_{l=1}^{12} \frac{\nabla \times S_{e_l}(\mathbf{r})}{-i\omega\mu} \xi_{e_l} = \frac{1}{i\omega} \begin{bmatrix} (v_x^H)^T \xi \\ (v_y^H)^T \xi \\ (v_z^H)^T \xi \end{bmatrix} \tag{48}$$

This time the only non zero values of v_x^H, v_y^H, v_z^H are x, y and z components of

$$\left(\frac{\nabla \times S_{e_1}(\mathbf{r})}{-\mu}, \ldots, \frac{\nabla \times S_{e_{12}}(\mathbf{r})}{-\mu} \right)$$

As a result each component of the secondary electric and magnetic fields E, H at a specific receiver location may be represented using

$$v^T \xi = v^T \left[(\tilde{A} + \mathrm{i}\omega \tilde{B})^{-1} g \right] \tag{49}$$

where v is a real valued vector, $g = g(\omega)$ is complex valued and $g(\omega)$ should be changed to $\frac{g}{\mathrm{i}\omega}$ in the case of H. The calculation is done in such a way that the quantity in square brackets is evaluated first and then it is multiplied by v^T. This gives us the values of the electric and magnetic secondary fields at a receiver location, which is sufficient to calculate the MT response at this location.

Magnetotelluric response Z, K is a smooth function of frequency, so it may be efficiently interpolated between frequencies. Such an interpolation has been considered in the literature [38]. In Fig. 1 we present values of Z_{xx} in the complex plane when the frequency is changed. One can see that Z_{xx} is a quite complicated function of frequency, so that the piecewise linear or high order polynomial interpolation is not accurate enough. Rational interpolation through the model order reduction, which is the topic of the current paper, gives a more accurate approximation.

Remark 1 Another advantage of using an interpolation based on the model order reduction is its independence on the magnitude of the source term in Eq. 39. Using a reasoning similar to the one in the proof of Theorem 3, one can show that if in the formulas for numerical approximation of electric (47) and magnetic (48) fields, we

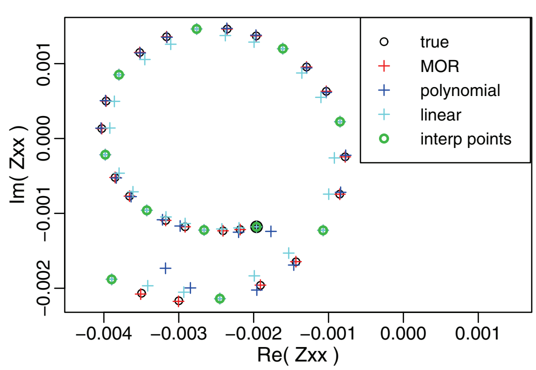

Fig. 1 Z_{xx} in the complex plane for the model considered in Section 5 for 31 frequencies log-uniformly distributed in the interval [1Hz, 1000Hz]. True values are shown together with the high order polynomial, piecewise linear and model order reduction interpolation. Every third value (shown by *green cirlces*) is used as an interpolation point

use approximation $\tilde{h}_{\tilde{V}}(\mathrm{i}\omega)$ instead of ξ, then the values of Z, K do not depend on the magnitude of $\tilde{b}$.

3.2 Null space of A and divergence correction

The proposed approach is very efficient when the representation of the null space allows $\tilde{K}^*\tilde{B}\tilde{K}$ to be sparse. This is true in the considered application as the null space of the curl $\nabla\times$ is the range of the gradient ∇.

Let $\mathcal{H}_0^{1,h}(\Omega)$ be a space spanned by the nodal shape functions on the same mesh as is used for edge element approximation of the electric field E with Eq. 39. The null space of $\tilde{A}$, which is the null space of the curl operator $\nabla\times$, is the range of the gradient operator ∇ acting on $\mathcal{H}_0^{1,h}(\Omega)$ (see Appendix B in [16]). To explain this more precisely, let φ be a scalar field defined at the vertices inside the domain Ω ($\varphi = 0$ on $\partial\Omega$), $\varphi \in \mathcal{H}_0^{1,h}(\Omega)$. Then $\nabla\varphi$ is defined at the edges of the mesh of Ω. Let edge e point from vertex v_1 to vertex v_2, then the operator ∇ acts on φ in such a way, that

$$(\nabla\varphi)(e) = \varphi(v_2) - \varphi(v_1)$$

Let N_v be the number of vertices inside Ω and let $(\psi_j)_{j=1}^{N_v}$ be nodal shape functions. We define $\tilde{K}$ as a matrix with entries $1, -1$ such that for $\varphi = \sum_{j=1}^{N_v} \eta_j \psi_j$

$$((\nabla\varphi)(e_k))_{k=1}^{N} = \tilde{K}\eta \tag{50}$$

Notice that, using Eq. 23

$$K^*K = \tilde{K}^*\tilde{B}\tilde{K} = \left[\int_\Omega \sigma \nabla\psi_i \cdot \nabla\psi_j\right]_{i,j=1}^{N_v} \tag{51}$$

Thus finding $(K^*K)^{-1}K^*b = (\tilde{K}^*\tilde{B}\tilde{K})^{-1}\tilde{K}^*\tilde{b}$, which is needed to obtain b_W of Eq. 31, requires to solve the Poisson equation with σ as the coefficient (see Eq. 53 below). Matrix (51) is real valued. Moreover the number of vertices N_v is more than three times less than the number of edges N, so finding $(K^*K)^{-1}K^*b$ is more than 10 times faster than evaluating $\tilde{h}(s)$ for one value of s.

The procedure above is strongly related to divergence correction [11, 24, 30, 36, 37, 39]. Consider Sobolev spaces defined below:

$$\begin{aligned}
\mathcal{H}_0^1(\Omega) &= \{\psi : \Omega \to \mathbb{C},\ \textstyle\int_\Omega \left(|\psi|^2 + |\nabla\psi|^2\right) < \infty,\ \psi|_{\partial\Omega} = 0\} \\
R(\nabla) &= \{\nabla\psi,\ \psi \in \mathcal{H}_0^1(\Omega)\} \\
R(\nabla)^{\perp_\sigma} &= \{F \in \mathcal{H}_0(\nabla\times, \Omega),\ \textstyle\int_\Omega \sigma F \cdot \nabla\psi = 0 \ \ \forall\psi \in \mathcal{H}_0^1(\Omega)\}
\end{aligned} \tag{52}$$

If an error $\nabla\varphi$, $\varphi \in \mathcal{H}_0^1$, is added to E, only the second term in Eq. 39 is affected. As a result if φ is non-zero only in a region where σ is small, then the change in the residual will be small, especially for low frequency ω. This shows that the residual is not sensitive to perturbing the electric field by a potential field in regions of low conductivity σ. Thus the calculation of E is an ill-posed problem. A regularization is provided by the divergence correction which corrects the value of the obtained field on the null space of the curl.

The null-space correction we propose, is analogous to the divergence correction. It calculates the values of the field on the null space exactly, interpolating only the part orthogonal to the null space. In this way, it provides a regularization to the ill-posed interpolation problem.

Using the Helmholtz decomposition, Eq. 39 for the electric field E can be decomposed into two uncoupled equations [24]

$$\begin{aligned} \int_\Omega \frac{1}{\mu}\nabla\times E_\perp\cdot\nabla\times F_\perp + \mathrm{i}\omega\int_\Omega \sigma E_\perp\cdot F_\perp &= \int_\Omega -\mathrm{i}\omega(\sigma-\sigma^p)E^p\cdot F_\perp \\ \mathrm{i}\omega\int_\Omega \sigma\nabla\varphi_E\cdot\nabla\psi &= \int_\Omega -\mathrm{i}\omega(\sigma-\sigma^p)E^p\cdot\nabla\psi \end{aligned} \tag{53}$$

where the test functions in Eq. 53 are $F_\perp \in R(\nabla)^{\perp_\sigma}$, $\psi \in \mathcal{H}_0^1(\Omega)$. The representation of the electric field E as $E = E_\perp + \nabla\varphi_E$ is the Helmholtz decomposition into the part in the null space of the curl: $\nabla\varphi_E \in R(\nabla) = N(\nabla\times)$ for $\varphi_E \in \mathcal{H}_0^1(\Omega)$, and the part orthogonal to it $E_\perp \in R(\nabla)^{\perp_\sigma}$.

Enforcing E to satisfy the second equation in Eq. 53 is called divergence correction. Using the discrete space of the edge elements $\mathcal{H}_0^h(\nabla\times,\Omega)$ and the nodal elements on the same mesh $\mathcal{H}_0^{1,h}(\Omega)$ in Eqs. 52 and 53 results in a method for the correction of the field in the discrete setting. In this case the decomposition of the Eq. 39 into Eq. 53 corresponds to the decomposition of Eq. 27 into two uncoupled Eq. 28.

Divergence correction has been shown to be essential in the convergence of iterative solvers [11, 30, 36, 37, 39]. It is a part of multigrid preconditioners for Maxwell's equations [19, 21]. It is also helpful in removing an error from a solution obtained using a direct solver [24]. The error in this case is due to insufficient precision used by the solver. When $\tilde{b}$ does not depend on s, applying the null space correction adds numerical stability. This effect is shown by our numerical experiment (see Section 5).

Considering the null space of curl operator in Maxwell's equations is important not only for electromagnetic geophysical soundings, but in all situations where the frequency is low and/or there is a region of low electrical conductivity, for example in the problem of computation of interior resonances of cavities where the null space correction might allow to avoid spurious modes.

4 The adaptive choice of shifts

In this section we discuss an adaptive algorithm, when the interpolating shifts $(s_j)_{j=1}^n$ are added one by one to enlarge $\tilde{V}$.

4.1 Theory

Let us assume that the shifts are chosen from a compact set $I \subset \mathbb{C}$ such that $I \cap (-\infty, 0] = \varnothing$. Assume that the n shifts $s_1, \ldots, s_n \in I$ have been chosen already and consider the choice of the shift s_{n+1}. The relative error of approximation

$$\mathrm{RE}(s) = \frac{||\tilde{h}(s) - \tilde{h}_{\tilde{V}}(s)||_2}{||\tilde{h}(s)||_2}$$

is not known, so we use an error indicator $\mathrm{EI}(s)$, which is nonnegative for $s \in I$ and is an approximation of the relative error:

$$\mathrm{EI}(s) \approx \mathrm{RE}(s) \qquad \text{for } s \in I$$

The next interpolating shift is chosen as the maximizer of the error indicator over the set I:

$$s_{n+1} = \mathrm{argmax}_{s \in I} \ \mathrm{EI}(s) \tag{54}$$

The algorithm stops, when the approximation is good enough.

We are interested if it may happen that $\tilde{V}$ becomes rank deficient when an additional shift is added. The next lemma says that adding $\tilde{h}(s_*)$ to the $\mathrm{colsp}(\tilde{V})$ will make $\tilde{V}$ rank deficient if and only if the approximation $\tilde{h}_{\tilde{V}}(s)$ is exact for $s = s_*$.

Lemma 1 *Let $\tilde{V}$ satisfying* Eq. 3 *be full rank, then*

$$\tilde{h}(s_*) \in colsp(\tilde{V}) \iff \tilde{h}_{\tilde{V}}(s_*) = \tilde{h}(s_*) \tag{55}$$

Proof According to the definition of $\tilde{h}_{\tilde{V}}$, it is always true that $\tilde{h}_{\tilde{V}} \in \mathrm{colsp}(\tilde{V})$, so the direction "$\Leftarrow$" is trivial.

To prove "$\Rightarrow$", notice that $\tilde{h}(s_*) \in \mathrm{colsp}(\tilde{V})$ means that $\tilde{h}(s_*) = \tilde{V}\beta_*$ for some $\beta_* \in \mathbb{C}^n$. This implies that for $s = s_*$ Eq. 6 is satisfied by $\beta = \beta_*$. As a result $\tilde{h}_{\tilde{V}}(s_*) = \tilde{V}\beta_*$, which implies $\tilde{h}_{\tilde{V}}(s_*) = \tilde{h}(s_*)$. □

The next theorem says that for a reasonable error indicator, the adaptive algorithm cannot fail.

Theorem 4 *Let the error indicator satisfy*

$$\forall s \in I \quad \tilde{h}_{\tilde{V}}(s) = \tilde{h}(s) \Rightarrow EI(s) = 0 \tag{56}$$

If the adaptive algorithm stops whenever

$$\max_{s \in I} \ EI(s) = 0 \tag{57}$$

then $\tilde{V}$ cannot become rank deficient.

Proof Assume that $\tilde{V}$ is full rank, but adding $\tilde{h}(s_{n+1})$ would make it rank deficient. Lemma 1 implies that $\tilde{h}_{\tilde{V}}(s_{n+1}) = \tilde{h}(s_{n+1})$, which together with Eq. 56 implies that $\mathrm{EI}(s_{n+1}) = 0$. As s_{n+1} is a maximizer of EI for $s \in I$, then it must be that Eq. 57 is satisfied and thus the algorithm stops at iteration n, so s_{n+1} is not added and $\tilde{V}$ does not become rank deficient. □

Notice that reasonable error indicators, like the residual norm or the relative residual norm satisfy assumption (56).

If we assume analyticity of $\tilde{b}(s)$, then the assumption (56) is not needed, thus one could choose shifts in an arbitrary way and at each iteration either the approximation is exact for all points in $s \in I$ or there is at most a finite number of values of the next interpolating shift s_{n+1} that could make $\tilde{V}$ rank deficient. This is expressed in the following theorem.

Theorem 5 *Assume that I is connected and that vector $\tilde{b}(s)$ has entries that are analytic on I. If $\tilde{V}$ is full rank and*

$$\tilde{h}_{\tilde{V}}(s) \neq \tilde{h}(s) \text{ for some } s \in I \tag{58}$$

then there is at most a finite number of points $s_* \in I$ such that $\tilde{h}(s_*) \in colsp(\tilde{V})$.

Proof Recall that a function is analytic on compact set I, if there is an open set, containing I, in which the function is analytic. Assuming that the entries of $b(s)$ are analytic on I using the definition of $\tilde{h}$, Eq. 1, one can conclude that the entries of $\tilde{h}(s)$ are analytic on I (one could also use Eq. 17).

Consider a matrix with $\tilde{h}(s_1), \tilde{h}(s_2), \ldots, \tilde{h}(s_n), \tilde{h}(s)$ as columns:

$$C(s) = \left[\ \tilde{h}(s_1)\ \ \tilde{h}(s_2)\ \ \ldots\ \ \tilde{h}(s_n)\ \ \tilde{h}(s)\ \right] \tag{59}$$

Assume that there are infinitely many points $s_* \in I$ such that $\tilde{h}(s_*) \in \text{colsp}(\tilde{V})$. Using Eq. 3 this means that there are infinitely many points $s_* \in I$ such that $C(s_*)$ is rank deficient. Consider an arbitrary $n \times n$ submatrix $C_M(s)$ of $C(s)$. Its determinant

$$a(s) = det(C_M(s))$$

is an analytic function of $s \in I$ as a linear combination of analytic entries of $\tilde{h}(s)$. As $C(s_*)$ is rank deficient for infinitely many points $s_* \in I$, then a has infinitely many zeroes in I. As I is compact, then there must be a sequence of zeros $z_n \in I$ convergent to $z_0 \in I$. So a is equal to 0 in the vicinity of z_0 and as I is connected, then

$$a(s) = 0 \text{ for all } s \in I$$

We have proven that for any $s \in I$ the determinant of an arbitrary $n \times n$ submatrix of $C(s)$ is equal to 0. Thus for an arbitrary $s \in I$ matrix $C(s)$ is rank deficient. With the assumption that $\tilde{V}$ is full rank, the first n columns of $C(s)$ are linearly independent, so it must be that for an arbitrary $s \in I$

$$\tilde{h}(s) \in \text{span}\left\{\tilde{h}(s_1), \tilde{h}(s_2), \ldots, \tilde{h}(s_n)\right\} = \text{colsp}(\tilde{V})$$

which, using Lemma 1, contradicts assumption (58).

□

4.2 Algorithm

In this section, we present an algorithm for choosing the interpolating shifts s_j. We will consider the values of the shifts in an interval I in the complex plane. The best choice of shifts would be such that minimizes the maximum relative error of approximation over interval $\{s = \mathrm{i}\omega : \omega \in [\omega_{\min}, \omega_{\max}]\}$, since the transfer function values are needed in this interval:

$$\min_{s_1,\ldots,s_n\in I} \max_{\omega\in[\omega_{\min},\omega_{\max}]} \frac{\|\tilde{h}(\mathrm{i}\omega) - \tilde{h}_{\tilde{V}}(\mathrm{i}\omega)\|_2}{\|\tilde{h}(\mathrm{i}\omega)\|_2} \tag{60}$$

Such an approach is not pursued in this paper for two reasons. Firstly because the true relative error of approximation is not known, so we have to use an error indicator $\mathrm{EI}_{(s_1,\ldots,s_n)}(\mathrm{i}\omega)$. Secondly, if Eq. 60 were used, the n-th step optimal shifts would most likely not appear among the $n+1$ optimal shifts.

Because of that we consider an approach in which at each iteration, given $(s_1, \ldots, s_n)$, we will add one value s_{n+1} in order to form $(s_1, \ldots, s_n, s_{n+1})$. Also we assume that $I = \{s = \mathrm{i}\omega : \omega \in [\omega_{\min}, \omega_{\max}]\}$ and we use the fact that at each interpolation shift s_j, the interpolation is exact, so the error of approximation is 0, thus the value of the next interpolation shift s_{n+1} is chosen at the maximum of the error indicator function $\mathrm{EI}_{(s_1,\ldots,s_n)}(s)$ for $s \in I$:

$$s_{n+1} = \mathrm{argmax}_{s\in I} \ \mathrm{EI}_{(s_1,\ldots,s_n)}(s) \tag{61}$$

In such a way, we set the error to 0 at the location that needs it the most, the location at which the error is the largest.

In the case when b does not depend on s, as for the approximation of the Jacobian [23], we consider two intervals to choose the shifts from: the purely imaginary interval $\{\mathrm{i}\omega : \omega \in [\omega_{\min}, \omega_{\max}]\}$ and a purely real interval $[\lambda_{\min}, \lambda_{\max}]$, containing non-zero eigenvalues of A. For the forward problem approximation considered in the current paper, when $\tilde{b}$ is complex valued and depends on the shift s we approximate it in the interval $\{\mathrm{i}\omega : \omega \in [\omega_{\min}, \omega_{\max}]\}$.

The norm of the residual of Eq. 2 may be used as the error indicator [6, 23, 40]. Yet in the considered case, it is more natural to use the relative residual norm. This makes our algorithm not dependent on the magnitude of the source term $\tilde{b}(s)$ (compare with Theorem 3). Also in the case of $\tilde{b}$ not dependent of the shift s, the residual norm can be explicitly calculated using formula of Theorem 2.4 in [23] which is not valid for the case of $\tilde{b}$ dependent on s. This makes the evaluation of the residual norm more expensive in this case.

Indeed, in order to find β, the solution of Eq. 6, one can use the precomputed $\tilde{V}^*\tilde{A}\tilde{V}$, $\tilde{V}^*\tilde{B}\tilde{V}$, but for each s one needs to evaluate $\tilde{V}^*\tilde{b}(s)$, which has a cost of order $O(nN)$. To calculate the relative residual of the approximation, we evaluate

$$\frac{\|\tilde{B}_d^{-\frac{1}{2}}(([\tilde{A}\tilde{V}] + s[\tilde{B}\tilde{V}])\beta - \tilde{b}(s))\|_2}{\|\tilde{B}_d^{-\frac{1}{2}}\tilde{b}(s)\|_2} \tag{62}$$

for precomputed $[\tilde{A}\tilde{V}]$, $[\tilde{B}\tilde{V}]$. Here $\tilde{B}_d$ is the diagonal of $\tilde{B}$. The most expensive part is the evaluation of $([\tilde{A}\tilde{V}]+s[\tilde{B}\tilde{V}])\beta$, which has numerical complexity $O(nN)$. This tells us that the numerical cost of the evaluation of the error indicator (62) is of order $O(nN)$ for each s.

Also, as was mentioned before, in magnetotellurics there is a number of frequencies of interest $\breve{\omega}_1, \ldots, \breve{\omega}_p$. We propose an algorithm that considers the values of interpolating shifts only in the set $\{i\check{\omega}_1, \ldots, i\check{\omega}_p\}$, for p small. The algorithm is presented below

Algorithm 1 AIRD (Adaptive choice of Imaginary shifts; norm of the Residual as the error indicator; $\tilde{b}$ Dependent on s)

1. Set $n = 2$, choose $\omega_1 = \omega_{\min}$, $\omega_2 = \omega_{\max}$ and set $\tilde{V}_{1:2}$ as
$$\operatorname{colsp}(\tilde{V}_{1:2}) = \operatorname{span}\left\{(\tilde{A} + i\omega\tilde{B})^{-1}\tilde{b} : \omega \in \{\omega_1, \omega_2\}\right\}$$
2. Find ω_{n+1} as the maximizer of the (scaled) relative residual norm
$$\frac{\|\tilde{B}_d^{-\frac{1}{2}}((\tilde{A} + i\omega\tilde{B})\tilde{h}_{\tilde{V}}(i\omega) - \tilde{b}(i\omega))\|_2}{\|\tilde{B}_d^{-\frac{1}{2}}\tilde{b}(i\omega)\|_2} \tag{63}$$
over $\omega \in \{\check{\omega}_1, \ldots, \check{\omega}_p\}$.
3. Set $\tilde{V}_{1:(n+1)}$ as
$$\operatorname{colsp}(\tilde{V}_{1:(n+1)}) = \operatorname{colsp}(\tilde{V}_{1:n}) \oplus \operatorname{span}\{(\tilde{A} + i\omega_{n+1}\tilde{B})^{-1}\tilde{b}\}$$
4. If exit criteria met(approximation is good enough), stop
5. Set $n = n + 1$ and jump to 2

As only a fixed number of shifts is considered, we can apply the null space correction. As a first step, one evaluates the null space part $\tilde{h}_{\tilde{K}}(i\check{\omega}_1), \ldots, \tilde{h}_{\tilde{K}}(i\check{\omega}_p)$, and then constructs the model order reduction approximation to $\tilde{h}_{\tilde{W}}(s)$.

5 Numerical results

In order to test the proposed method we use the forward solver of [24]. We consider a model presented in Fig. 2 with a 3d hill and a 3d valley. There is a conductive (1Ωm) object below the earth's surface in 50Ωm background. The conductive object is placed at $[-700\text{m}, 700\text{m}] \times [-328.3\text{m}, 328.3\text{m}]$ in XY plane and extends from approximately 450m to 1150m in depth. YZ cross-section plotted in Fig. 3 shows the location of the object. The air is approximated by $10^7\,\Omega$m and the term $i\omega\epsilon$ is dropped completely in all of the domain. In the numerical test we consider the magnetotelluric response Z, K at one receiver location at the bottom of the valley, marked by a blue point in Fig. 2. We are interested in the response $\tilde{h}(i\omega)$ for a range of frequencies considered in magnetotellurics $\frac{\omega}{2\pi} \in [0.01\text{Hz}, 1000\text{Hz}]$. The hexahedral mesh consists of 31, 31 and 25 elements in x, y and z directions, respectively, and it extends to 45km from the center in x and y directions. In z direction it extends to 32km above the surface and 47km deep. The system matrix has 67,140 columns and the same number of rows. The total number of elements is 24,025 and the total number of edges inside the domain is 67,140.

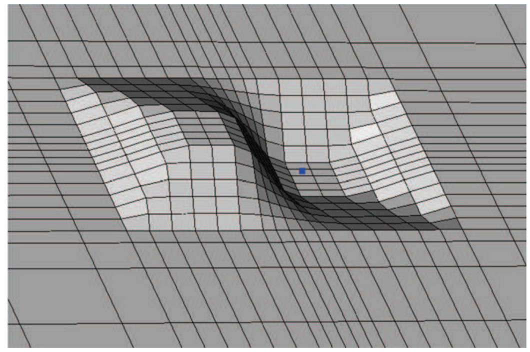

Fig. 2 The central part of the surface mesh, together with the location of the receiver shown by a blue point

514 Let us consider the edge element approximation of the forward MT response with $\tilde{b}(i\omega) = g(\omega)$, where $g(\omega)$ defined in Eq. 43, depends on the primary plane wave field. Usually in MT, one considers two cases: E field purely in x direction(with H purely in y direction) and E field purely in y direction (with H purely in x direction).

518 As the source in Eq. 39, which is the primary plane wave electric field multiplied by the conductivity difference $(\sigma - \sigma^p)E^p$, is not divergence free, the vector $b(i\omega)$ is not orthogonal to the null space of A. Moreover, its part $\tilde{b}_{\tilde{K}}(s)$ lying in the null space depends on s. To deal with this problem we apply the developed method of the null space correction.

523 To compare the quality of approximations we calculate the maximum relative error of an approximation

$$\max_{\omega\in[\omega_{\min},\omega_{\max}]} \frac{\|\tilde{h}_{\tilde{V}}(i\omega) - \tilde{h}(i\omega)\|_2}{\|\tilde{h}(i\omega)\|_2} \tag{64}$$

525 We also calculate the maximum of the relative residual norm:

$$\max_{\omega\in[\omega_{\min},\omega_{\max}]} \frac{\|(A+i\omega I)h_V(i\omega)-b\|_2}{\|b\|_2} \approx \max_{\omega\in[\omega_{\min},\omega_{\max}]} \frac{\|\tilde{B}_d^{-\frac{1}{2}}\left[(\tilde{A}+i\omega\tilde{B})\tilde{h}_{\tilde{V}}(i\omega)-\tilde{b}\right]\|_2}{\|\tilde{B}_d^{-\frac{1}{2}}\tilde{b}\|_2} \tag{65}$$

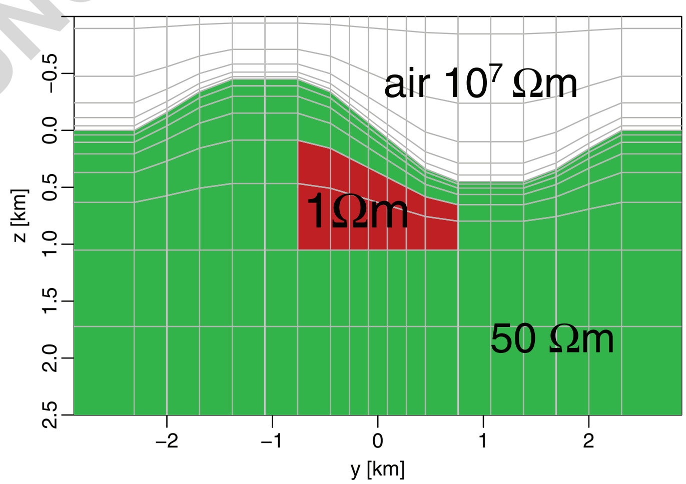

Fig. 3 The central part of the YZ cross-section at x=0

We consider algorithm AIRD for $p = 31$ frequencies of interest in the range $[\omega_{\min}, \omega_{\max}]$. In Fig. 4, we present the maximum of the relative error over the whole interval $[\omega_{\min}, \omega_{\max}]$ and the maximum of the relative residual norm over the same interval as a function of the iteration number n. At each iteration the approximation obtained with the null space correction is more than an order of magnitude more accurate than without the correction. The max relative error of approximation is decreased to 10^{-7} in 25 iterations, which is about two orders of magnitude more accurate than without the correction. For n larger than 25, we can see a stagnation caused by constraining the interpolation frequencies to the set $\{\check{\omega}_1, \ldots, \check{\omega}_{31}\}$.

To test the efficiency of the model order reduction we used three-dimensional low frequency Maxwell's equation solver that uses deformed hexahedral edge finite elements and direct solvers parallelized on SMP computers [24, 25]. The code has been developed for magnetotellurics applications and tested on synthetic and real-world examples. The proposed model order reduction offers largest speedup for an iterative solver [21, 28] if $\tilde{h}_{\tilde{V}}$ is used as a starting point. As demonstrated in Fig. 4, in the case of calculation of $\tilde{h}$ for 30 frequencies with relative residuals no larger than 10^{-5}, the speedup from using the model order reduction is 2 times. The speedup is higher if more frequencies are considered. For example, for 60 frequencies, the speedup is 4 times.

The presented calculation of the speedup takes into account only the relative residual, which has similar values for the algorithm with and without the null space correction. Applying the null space correction leads to an additional speedup of 30 % if one stops the iteration at the same level of the maximum relative error.

Figure 5 presents the results of using the suggested null space correction method for a different case. In this simulation $\tilde{b}$ does not depend on s. For choosing the interpolation shifts we use the AIR algorithm [23], which is similar to AIRD, discussed in the current paper, but developed for $\tilde{b}$ not dependent on s. In this case, the interpolation shifts may be anywhere in the interval I. The comparison of the algorithm with

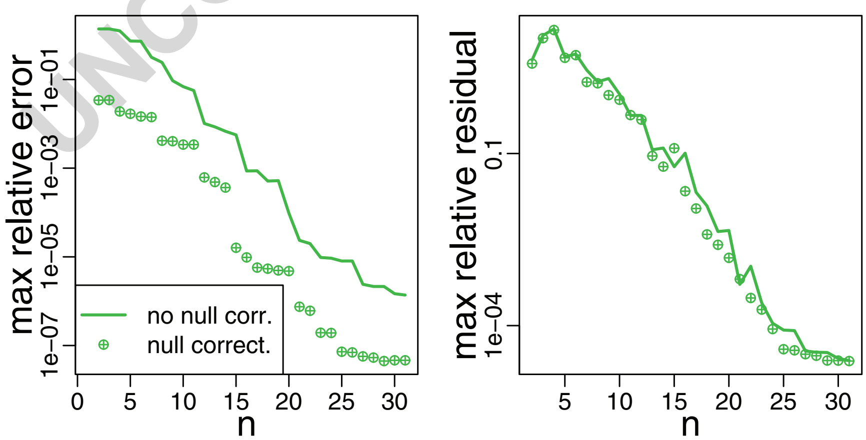

Fig. 4 The relative error (*left*) and the relative residual (*right*) as a function of the iteration number n for AIRD for the case of the forward problem with the source plane wave with E purely in x direction. Comparison of the strategy with the null space correction (shown by ⊕ symbol) and without the null space correction (shown by a *solid line*) is presented

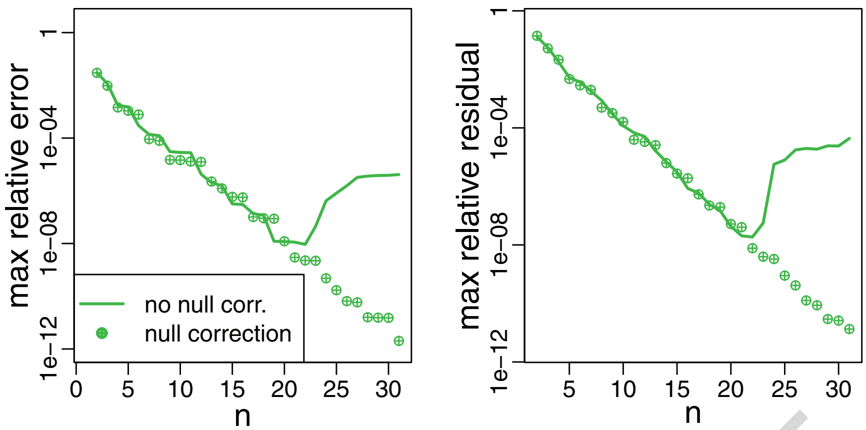

Fig. 5 The relative error (*left*) and the relative residual (*right*) as a function of the iteration number n for AIR strategy in the case of $\tilde{b}$ not dependent on s. Comparison of the strategy with the null space correction (shown by $\oplus$ symbol) and without the null space correction (shown by a *solid line*) is presented

and without the null space correction is presented in Fig. 5. The calculation was done for the case of $\tilde{b} = v_x$ for v_x defined in Eq. 47, which is used in the calculation of the Jacobian of x component of the electric field E. In the case of $\tilde{b}$ not dependent on s, the null space part of the transfer function satisfies $h_K(s) = \frac{1}{s}h_K(1)$, so applying the null space correction is comparable to adding a single vector $h_K(1)$ to the column space of V. Figure 5 shows that when the null space correction is applied, at initial stage of the iteration the speed of decreasing of the maximum relative error does not show a significant improvement over the algorithm without the correction. However, the overall behavior and stability of the algorithm changes drastically. The algorithm with the null space correction reduces the max relative error to a much smaller value, in 25 iterations the maximum error is four orders of magnitude smaller than without the correction. The null space correction regularizes the ill-posed interpolation problem in a similar way the divergence correction regularizes the ill-posed problem of the calculation of the electric field. The regularization is done by constraining and proper evaluation of the null space components. It allows to turn a semiconvergent algorithm into a convergent one.

For the case of $\tilde{b}$ dependent on s (see Fig. 4) the regularization provided by the null space correction manifests itself in a significant reduction of the approximation error without any reduction of the residual norm (shown in Fig. 4 right). In a similar way, divergence correction removes the error in the approximated electric field E which is not seen in the values of the residual [24].

6 Conclusions

The paper extends model order reduction method for the transfer function to the case when the matrix has a non-empty null space and the right hand side depends on the shift. We propose the null-space correction method, which allows to correct the solution in the part lying in the null space of the operator. Our numerical tests show that the method reduces the approximation error by two to four orders of magnitude. We also develop a method of adaptive choice of shifts and prove that the algorithm never fails. In application to a forward low frequency electromagnetic problem, the developed methods allow to significantly speed up the calculations without any loss of accuracy.

References

1. Antoulas, A.C., Sorensen, D.C., Gugercin, S.: A survey of model reduction methods for large-scale systems. Contemp. Math. **280**, 193–220 (2001)
2. Bai, Z.: Krylov subspace techniques for reduced-order modeling of large-scale dynamical systems. Appl. Numer. Math. **43**, 9–44 (2002)
3. Benner, P., Mehrmann, V., Sorensen, D.C.: Dimension Reduction of Large-Scale Systems, vol. 45. Springer (2005)
4. Bodendiek, A., Bollhöfer, M.: Adaptive-order rational Arnoldi-type methods in computational electromagnetism. BIT Numer. Math. 1–24 (2013)
5. Boerner, R.U.: Numerical modelling in geo-electromagnetics: advances and challenges. Surv. Geophys. **31**, 225–245 (2010)
6. Druskin, V., Lieberman, C., Zaslavsky, M.: On adaptive choice of shifts in rational Krylov subspace reduction of evolutionary problems. SIAM J. Sci. Comput. **32**(5), 2485–2496 (2010)
7. Druskin, V., Simoncini, V.: Adaptive rational Krylov subspaces for large-scale dynamical systems. Syst. Control Lett. **60**(8), 546–560 (2011)
8. Druskin, V., Simoncini, V., Zaslavsky, M.: Solution of the time-domain inverse resistivity prolem in the model reduction framework part I: one-dimensional problem with SISO data. SIAM J. Sci. Comput. **35**(3), A1621–A1640 (2013)
9. Elman, H.C., Meerbergen, K., Spence, A., Wu, M.: Lyapunov inverse iteration for identifying Hopf bifurcations in models of incompressible flow. SIAM J. Sci. Comput. **34**(3), A1584–A1606 (2012)
10. Everett, M.E.: Theoretical developments in electromagnetic induction geophysics with selected applications in the near-surface. Surv. Geophys. **33**, 29–63 (2012)
11. Farquharson, C.G., Meinsopust, M.: Three-dimensional finite-element modeling of magnetotelluric data with a divergence correction. J. Appl. Geophys. **75**, 699–710 (2011)
12. Freund, R.W.: Model reduction methods based on Krylov subspaces. Acta Numer. **12**, 267–319 (2003)
13. Gallivan, K., Grimme, G., Van Dooren, P.: A rational Lanczos algorithm for model reduction. Numer. Algoritm. **12**(1), 33–63 (1996)
14. Grimme, E.J.: Krylov Projection Methods for Model Reduction. Ph.D. thesis, University of Illinois, Urbana-Champaigne (1997)
15. Gugercin, S., Antoulas, A.C., Beattie, C.: H_2 model reduction for large-scale linear dynamical systems. SIAM J. Matrix Anal. Appl. **30**(2), 609–638 (2008)
16. Gunzburger, M.D., Bochev, P.B.: Least-Squares Finite Element Methods. Springer, New York (2009)
17. Güttel, S.: Rational Krylov approximation of matrix functions: Numerical methods and optimal pole selection. GAMM-Mitteilungen **36**(1), 8–31 (2013)
18. Güttel, S., Knizhnerman, L.: A black-box rational Arnoldi variant for Cauchy–Stieltjes matrix functions. BIT Numer. Math. **53**(3), 595–616 (2013)
19. Hiptmair, R.: Multigrid method for Maxwell's equations. SIAM J. Numer. Anal. **36**(1), 204–225 (1998)
20. Knizhnerman, L., Druskin, V., Zaslavsky, M.: On optimal convergence rate of the rational Krylov subspace reduction for electromagnetic problems in unbounded domains. SIAM J. Numer. Anal. **47**(2), 953–971 (2009)
21. Kolev, T.V., Vassilevski, P.S.: Some experience with a H1-based auxiliary space AMG for H(curl) problems. Lawrence Livermore Nat. Lab., Livermore, CA, Rep. UCRL-TR-221841 (2006)
22. Kordy, M., Cherkaev, E., Wannamaker, P.: Variational formulation for Maxwell's equations with Lorenz gauge: Existence and uniqueness of solution. Int. J. Numer. Anal. Model. **12**(4), 731–749 (2015)

23. Kordy, M., Cherkaev, E., Wannamaker, P.: Adaptive model order reduction for the Jacobian calculation in inverse multi-frequency problem for Maxwell's equations. Applied Numerical Mathematics, accepted (2016)
24. Kordy, M., Wannamaker, P., Maris, V., Cherkaev, E.: Three-dimensional magnetotelluric inversion including topography using deformed hexahedral edge finite elements and direct solvers parallelized on SMP computers, Part I: Forward problem and parameter Jacobians. Geophys. J. Int. **204**(1), 74–93 (2016)
25. Kordy, M., Wannamaker, P., Maris, V., Cherkaev, E., Hill, G.J.: Three-dimensional magnetotelluric inversion including topography using deformed hexahedral edge finite elements and direct solvers parallelized on SMP computers, Part II: Direct data-space inverse solution. Geophys. J. Int. **204**(1), 94–110 (2016)
26. Levin, E., Saff, E.B.: Potential theoretic tools in polynomial and rational approximation. In: Harmonic Analysis and Rational Approximation, pp. 71–94. Springer (2006)
27. Moret, I.: Rational Lanczos approximations to the matrix square root and related functions. Numer. Linear Algebra Appl. **16**(6), 431–445 (2009)
28. Mulder, W.A.: A multigrid solver for 3D electromagnetic diffusion. Geophys. Prospect. **54**(5), 633–649 (2006)
29. Nédélec, J.C.: A new family of mixed finite elements in $\mathbf{R}^3$. Numer. Math. **50**(1), 57–81 (1986)
30. Newman, G.A., Alumbaugh, D.L.: Three-dimensional magnetotelluric inversion using non-linear conjugate gradients. Geophys. J. Int. **140**, 410–424 (2000)
31. Popolizio, M., Simoncini, V.: Acceleration techniques for approximating the matrix exponential operator. SIAM J. Matrix Anal. Appl. **30**(2), 657–683 (2008)
32. Ragni, S.: Rational Krylov methods in exponential integrators for European option pricing. Numer. Linear Algebra Appl. (2013)
33. Ralph-Uwe, B., Ernst, O.G., Spitzer, K.: Fast 3-D simulation of transient electromagnetic fields by model reduction in the frequency domain using Krylov subspace projection. Geophys. J. Int. **173**(3), 766–780 (2008)
34. Ransford, T.: Potential Theory in the Complex Plane, vol. 28. Cambridge University Press (1995)
35. Saff, E.B., Totik, V.: Logarithmic Potentials with External Fields, vol. 316. Springer (1997)
36. Sasaki, Y.: Full 3-D inversion of electromagnetic data on PC. J. Appl. Geophys. **46**, 45–54 (2001)
37. Siripunvaraporn, W., Egbert, G., Lenbury, Y.: Numerical accuracy of magnetotelluric modeling: a comparison of finite difference approximations. Earth Planets Space **54**, 721–725 (2002)
38. Siripunvaraporn, W., Egbert, G., Lenbury, Y., Uyeshima, M.: Three-dimensional magnetotelluric inversion: data-space method. Phys. Earth Planet Inter. **150**, 3–14 (2005)
39. Smith, J.: Conservative modeling of 3-D electromagnetic fields, Part II: Biconjugate gradient solution and an accelerator. Geophysics **61**(5), 1319–1324 (1996)
40. Villena, J.F., Silveira, L.M.: ARMS - automatic residue-minimization based sampling for multi-point modeling techniques. In: DAC'09 Proceedings of the 46th Annual Design Automation Conference, pp. 951–956 (2009)
41. Zaslavsky, M., Druskin, V., Abubakar, A., Habashy, T., Simoncini, V.: Large-scale Gauss-Newton inversion of transient CSEM data using the model order reduction framework. Geophysics **78**(4), E161–E171 (2013)